Title

Deficiency of Melanoma Differentiation–associated Protein 5 Results in Exacerbated Chronic Postviral Lung Inflammation

Journal

American Journal of Respiratory and Critical Care Medicine, 189(4)

ISSN

1073-449X

Authors

Kim, Won-keun
Jain, Deepika
Sánchez, Melissa D
et al.

Publication Date

2014-02-15

DOI

10.1164/rccm.201307-1338oc

Peer reviewed

ORIGINAL ARTICLE

Deficiency of Melanoma Differentiation–associated Protein 5 Results in Exacerbated Chronic Postviral Lung Inflammation

Won-keun Kim[1], Deepika Jain[1], Melissa D. Sánchez[1], Cynthia J. Koziol-White[2], Krystal Matthews[3], Moyar Q. Ge[2], Angela Haczku[2], Reynold A. Panettieri, Jr.[2], Matthew B. Frieman[3], and Carolina B. López[1]

[1]Department of Pathobiology, School of Veterinary Medicine, and [2]Department of Medicine, University of Pennsylvania, Philadelphia, Pennsylvania; and [3]Department of Microbiology and Immunology, School of Medicine, University of Maryland at Baltimore, Baltimore, Maryland

Abstract

Rationale: Respiratory viral infections can result in the establishment of chronic lung diseases. Understanding the early innate immune mechanisms that participate in the development of chronic postviral lung disease may reveal new targets for therapeutic intervention. The intracellular viral sensor protein melanoma differentiation–associated protein 5 (MDA5) sustains the acute immune response to Sendai virus, a mouse pathogen that causes chronic lung inflammation, but its role in the development of postviral chronic lung disease is unknown.

Objectives: To establish the role of MDA5 in the development of chronic lung disease.

Methods: MDA5-deficient or control mice were infected with Sendai virus. The acute inflammatory response was evaluated by profiling chemokine and cytokine expression and by characterizing the composition of the cellular infiltrate. The impact of MDA5 on chronic lung pathology and function was evaluated through histological studies, degree of oxygen saturation, and responsiveness to carbachol.

Measurements and Main Results: MDA5 deficiency resulted in normal virus replication and in a distinct profile of chemokines and cytokines that associated with acute lung neutropenia and enhanced accumulation of alternatively activated macrophages. Diminished expression of neutrophil-recruiting chemokines was also observed in cells infected with influenza virus, suggesting a key role of MDA5 in driving the early accumulation of neutrophils at the infection site. The biased acute inflammatory response of MDA5-deficient mice led to an enhanced chronic lung inflammation, epithelial cell hyperplasia, airway hyperreactivity, and diminished blood oxygen saturation.

Conclusions: MDA5 modulates the development of chronic lung inflammation by regulating the early inflammatory response in the lung.

Keywords: respiratory virus; chronic lung disease; innate immunity; paramyxovirus

At a Glance Commentary

Scientific Knowledge on the Subject: Hospitalizations due to chronic postviral lung inflammatory diseases remain a major health burden, and better understanding of the innate immune mechanisms driving these diseases is required for the development of suitable therapies. Cellular proteins specialized in recognizing the infecting pathogens play a critical role in establishing and directing the quality of the host immune response to infection. Little is known of the impact of these early immune elements on the development of chronic lung disease.

What This Study Adds to the Field: This work demonstrates that signaling by the viral sensor molecule melanoma differentiation–associated protein 5 (MDA5) is critical for protection from the development of severe chronic postviral lung disease. MDA5 modulates the quality of the inflammatory infiltrate, independently of the control of virus replication. MDA5 promotes the acute recruitment of neutrophils to the lung and regulates the accumulation of pathogenic alternatively activated macrophages that promote chronic lung disease.

(Received in original form July 22, 2013; accepted in final form January 3, 2014)

This work was supported by National Institutes of Health grants R01-AI083284 (C.B.L.), R01-AI095569 (M.B.F.), P01-HL114471 and P30-ES013508 (R.A.P.), R01-AI072197 (A.H.), and T32-HL007586 (C.J.K.-W.).

Author Contributions: W.K.: study design, data collection, data analysis, and manuscript preparation. D.J.: study design, data collection, and data analysis. M.D.S.: data analysis. C.J.K.-W.: data collection and data analysis. K.M.; data collection. M.Q.G.: data collection. A.H.: data analysis. R.A.P.: data analysis. M.B.F.: data analysis. C.B.L.: study design, data analysis, and manuscript preparation.

Correspondence and requests for reprints should be addressed to Carolina B. López, Ph.D., University of Pennsylvania, School of Veterinary Medicine, Department of Pathobiology, 380 South University Avenue, Hill 318, Philadelphia, PA 19104. E-mail: lopezca@vet.upenn.edu

This article has an online supplement, which is accessible from this issue's table of contents at www.atsjournals.org

Am J Respir Crit Care Med Vol 189, Iss 4, pp 437–448, Feb 15, 2014

Originally Published in Press as DOI: 10.1164/rccm.201307-1338OC on January 13, 2014
Internet address: www.atsjournals.org

Infection with respiratory syncytial virus or other common paramyxoviruses leads to the development and exacerbation of chronic lung conditions, including asthma, chronic obstructive pulmonary disease (COPD), and fibrosis, in susceptible individuals (1–3). Hospitalizations due to severe manifestations of these lung conditions after virus infections remain a major health burden. Better understanding of the mechanisms driving these diseases is required for the development of suitable therapies.

Recent evidence indicates that virus-induced chronic lung disorders are mostly driven by mechanisms of the innate immune system (4–9). For example, in mice, development of chronic airway disease after infection with Sendai virus (SeV) or severe acute respiratory syndrome virus is mediated by alternatively activated macrophages (AAMs) (7, 9), and associations between the presence of AAMs and the incidence of COPD and asthma have been reported in humans (7, 10).

Germline-encoded pattern recognition receptors (PRRs) are the first line of defense against infections. Among PRRs, the retinoic acid–inducible gene-I (RIG-I)-like receptors and the melanoma differentiation–associated protein 5 (MDA5) detect molecular motifs present in viral oligonucleotides. RIG-I and MDA5 signal through a common pathway mediated by the adaptor protein mitochondrial antiviral–signaling protein (MAVS) that culminates in the expression of type I IFNs and proinflammatory genes, including chemokines and cytokines, that recruit and activate leukocytes (11). According to current paradigms, RIG-I and MDA5 recognize distinct virus molecular motifs present in different families of viruses. However, accumulating evidence indicates that a number of viruses can be recognized by both intracellular sensors (12). For example, MDA5 is involved in sensing SeV (13, 14), a paramyxovirus that bears a negative sense RNA genome and was originally classified as a RIG-I trigger (15, 16). Whether RIG-I and MDA5 have unique nonredundant activities and whether any of these activities affects the development of chronic lung disease after viral infection is unknown.

SeV causes bronchiolitis and persistent airway hyperreactivity in mice, providing the best available experimental model for virus-induced chronic lung disease (7, 17). Here we show that MDA5 deficiency leads to an altered inflammatory environment in the lung and to a striking shift in the expression of neutrophil- and monocyte/lymphocyte-attracting chemokines. These alterations result in enhanced accumulation of AAMs, whereas viral clearance and type I IFN responses are unchanged. MDA5 knockout (KO) mice exhibited a significant chronic increase in mucus-producing goblet cells and in bronchial smooth muscle cell hyperplasia that associated with enhanced airway hyperresponsiveness and with an impaired ability to maintain blood oxygen saturation. Overall, this study shows that signaling by MDA5 modulates the accumulation of pathogenic AAMs in the lung and protects from the development of

Table 1: Sequences of Primers for Quantitative RT-PCR

Genes	Forward (*Sense, 5′–3′*)	Reverse (*Antisense, 5′–3′*)
Tuba1b	TGCCTTTGTGCACTGGTATG	CTGGAGCAGTTTGACGACAC3
Rps11	CGTGACGAAGATGAAGATGC	GCACATTGAATCGCACAGTC3
Ifnβ	AGATGTCCTCAACTGCTCTC	AGATTCACTACCAGTCCCAG3
Ifnα-2	CCTGTGCTGCGAGATCTTACT	GGTGGAGGTCATTGCAGAAT
Ifnγ	GACTGTGATTGCGGGGTTGT	GGCCCGGAGTGTAGACATCT
Ifit2	GCAGAAGATGAGTCCTTGGA	CCTCAGCTTCCCCTAAGCAT
Rsad2	GAGATTCTGCAAGGAGGAGCTA	TGTCGCAGGAGATAGCAAGA
Ifih1	CGATCCGAATGATTGATGCA	AGTTGGTCATTGCAACTGCT3
Ddx58	CAGACAGATCCGAGACACTA	TGCAAGACCTTTGGCCAGTT
Il-6	ACAGAAGGAGTGGCTAAGGA	CGCACTAGGTTTGCCGAGTA
Tnfα	TCACTGGAGCCTCGAATGTC	GTGAGGAAGGCTGTGCATTG
Il-1β	CCTCTGATGGGCAACCACTT	TTCATCCCCCACACGTTGAC
Il-10	TGTCCAGCTGGTCCTTTGTT	ACTGCACCCACTTCCCAGT
Il-13	GGCAGCATGGTATGGAGTGT	CCATGCAATATCCTCTGGGT
Il-27p28	GATTGCCAGGAGTGAACCTG	CGAGGAAGCAGAGTCTCTCAG
Cxcl1	GCACCCAAACCGAAGTCATA	CTTGGGGACACCTTTTAGCA
Cxcl5	AATGAGCCTCCAGCTCCGCA	CGGCAGCGTGAACAGCAACA
Ccl3	TGCCCTTGCTGTTCTTCTCT	GTGGAATCTTCCGGCTGTAG
Ccl5	GCAGCAAGTGCTCCAATCTT	CAGGGAAGCGTATACAGGGT
Arg I	GGAAAGCCAATGAAGAGCTG	GATGCTTCCAACTGCCAGAC
Nos2	ATGGAGACTGTCCCAGCAAT	GGCGCAGAACTGAGGGTA
IL-33	ACCCACGAAAAGATATTCACTAAAA	CAAGCAAGGATCTCTTCCTAGAAT
Tslp	CAGCATGGTTCTTCTCAGGA	CTCGAACTTAGCCCCTTTCA
Areg	TCCAAGATTGCAGTAGTAGCTGTC	CCCTGAAGTATCGTTTCCAAAG
IL-22	TGACACTTGTGCGATCTCTG	ACAGGGCAATGAGAAGCAG
Mmp12	CGAAATTGAAAGCAGAAATCAAC	GGGAATATATGCTCCTGGGATA
Csf3	CCCGAAGCTTCCTGCTTA	CAGCTTGTAGGTGGCACACA
Relmα	TATGAACAGATGGGCCTCCT	AGGCAGTTGCAAGTATCTCCA
Chi3l3/4	TCTGGGTACAAGATCCCTGAA	TCATATGGAGATTTATAGAGGGGACT
SeV *Np*	TGCCCTGGAAGATGAGTTAG	GCCTGTTGGTTTGTGGTAAG
IAV *Np*	CAGCCTAATCAGACCAAATG	TACCTGCTTCTCAGTTCAAG

long-term lung pathology during SeV infection. MDA5 also regulated the expression of neutrophil-attracting chemokines during infection with influenza virus, suggesting that this molecule may be critical for the establishment of the local inflammatory response to infection with a large group of respiratory viruses. Some of the results of these studies have been previously reported in the form of an abstract (18).

Methods

Mice

C57BL/6 mice were purchased from Taconic Farms (Germantown, NY). MDA5$^{-/-}$ mice (C57BL/6 background) were kindly provided by Dr. Marco Colonna (Washington University, St. Louis, MO). Mice were bred and maintained in our facilities. This study was performed in strict accordance with the recommendations in the Guide for the Care and Use of Laboratory Animals of the National Institutes of Health. The protocol (803173) was approved by the Institutional Animal Care and Use Committee, University of Pennsylvania Animal Welfare Assurance Number A3079-01.

Viruses and Infections

SeV strains 52 and Cantell and influenza virus PR8 were propagated and titrated in our laboratory as we have described (19, 20). A detailed description of this procedure can be found in the online supplement. Cells were infected with the indicated doses of median tissue culture infectious dose ($TCID_{50}$)/cell. Mice were infected intranasally with 10 ID_{50} of SeV strain 52 (10,000 $TCID_{50}$/mouse) after anesthesia.

Murine Bone Marrow–derived Dendritic Cell Preparation

Bone marrow–derived dendritic cells were prepared according to a standard protocol (21). The cells were used after 4 days of culture.

Lung Cell Separation

Lungs were flushed using media containing 2 mM L-glutamine (Life Technologies, Carlsbad, CA), 10% FBS (Thermo Scientific, Waltham, MA), 0.2% β-mercaptoethanol (Sigma-Aldrich, St. Louis, MO), 2% Pen/Strep (Life Technologies), 1% Collagenase (Liberase Blendzymes; Roche, Indianapolis, IN), and 0.00001% DNase I (Roche) in DMEM (Life Technologies) and incubated at 37°C for 50 minutes. After red blood cell lysis, single-cell suspensions were incubated with anti-mouse CD16/32 (BD Biosciences, San Jose, CA) followed by incubation with anti-mouse CD45.2 (clone: 104; eBioscience, San Diego, CA) at 4°C. Cells were then incubated with magnetic bead–conjugated anti-CD45.2 antibody (Miltenyi Biotec, Auburn, CA) and separated by magnetic-associated sorting.

Protein Concentration in Bronchoalveolar Lavage

Lungs were lavaged with 1 ml of sterile saline as previously described (22). Total protein in bronchoalveolar lavage (BAL) was measured from the cell-free fraction by Bradford assay (Thermo Scientific).

Real-Time Quantitative PCR

Total RNA was purified from lungs using TRIzol (Life Technologies). RNA was reversed transcribed using the High Capacity RNA to cDNA kit (Applied Biosystems; Life Technologies) and amplified with specific primers in the presence of Power SYBR Green PCR Master Mixture (Applied Biosystems; Life Technologies). Normalization was conducted based on levels of *Tuba1b* and *Rps11*. Primer sequences are shown in Table 1.

Flow Cytometry

Single-lung-cell suspensions were stained with the following antibodies: CD11b (M1/70), CD11c (N418), Ly6G (1A8), Ly6C (HK1.4), and F4/80 (BM8) (BD Biosciences); CD206 (MR5D3; AbD Serotec, Raleigh, NC); and CD45 (104; eBioscience). A detailed description of this procedure can be found in the online supplement.

Immunohistochemistry

Paraffin sections (5 μm) of fixed lung tissue were stained as previously described (9). A detailed description of this procedure can be found in the online supplement.

Histology

After lavage, the left lobe of the lung was inflated and fixed with 0.5 ml of 10%

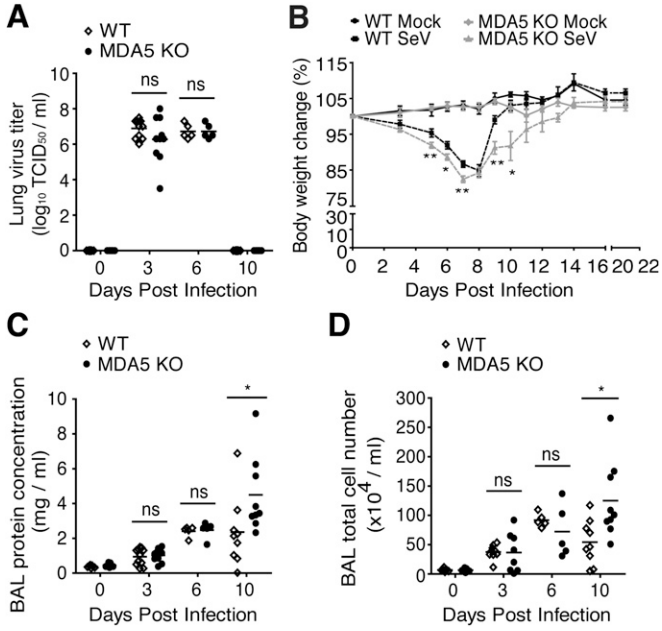

Figure 1. Melanoma differentiation–associated protein 5 (MDA5) deficiency enhances morbidity and tissue damage but does not affect virus replication. Wild-type (WT) and MDA5 knockout (KO) mice were infected with 10 ID_{50} of Sendai virus (SeV 52). (*A*) SeV titer was determined from lungs of infected mice at the indicated time points. (*B*) Body weight was monitored for 21 days after infection. Total protein concentration (*C*) and total cell numbers (*D*) in bronchoalveolar lavage (BAL) were examined by Bradford assay after 3, 6, and 10 days of infection. Data are representative of three independent experiments. $^*P < 0.05$ and $^{**}P < 0.01$ (unpaired Student's *t* test). ns = nonsignificant.

neutral-buffered formalin solution. Deparaffinized sections from fixed lungs were stained with hematoxylin and eosin. Lung inflammation was scored by a pathologist (M.D.S.). A detailed description of this procedure can be found in the online supplement. Goblet cells and mucus production were evaluated on slides stained with periodic acid-Schiff.

Pulse Oximetry

The MouseOx Pulse-oxymeter (Starr Life Sciences, Holliston, MA) was used to measure blood saturation of peripheral oxygen (Sp_{O_2}) in SeV-infected mice. A detailed description of this procedure can be found in the online supplement. Pa_{O_2} was estimated from Sp_{O_2} using the Ventworld interactive oxyhemoglobin dissociation curve tool, assuming a normal blood pH and arterial P_{CO_2} (23).

Measurement of Lung Hyperreactivity

SeV-infected mice were killed on Day 49 after infection for preparation of precision-cut lung slices containing an intrapulmonary small airway as previously described (24). A more extensive description of this procedure can be found in the online supplement.

Statistical Analyses

Statistical analyses were performed as indicated in each figure. GraphPad Prism version 5.00 for Windows (GraphPad Software, San Diego, CA) was used for analysis.

Results

MDA5 Protects from Morbidity and Respiratory Epithelium Damage Independently of Virus Clearance

To determine whether MDA5 has a protective role in the lung independent of controlling virus replication, we infected wild-type (WT) and MDA5 KO mice with 10 ID_{50} of SeV strain 52 (10^4 $TCID_{50}$), the minimal dose of virus to achieve 100% infection. Virus titers in the respiratory tract of WT and MDA5 KO mice were comparable on Days 3 and 6 after infection, and the virus was cleared by Day 10 (Figure 1A). However, MDA5 KO mice lost more weight and showed delayed recovery compared with WT mice (Figure 1B). To assess the integrity of the

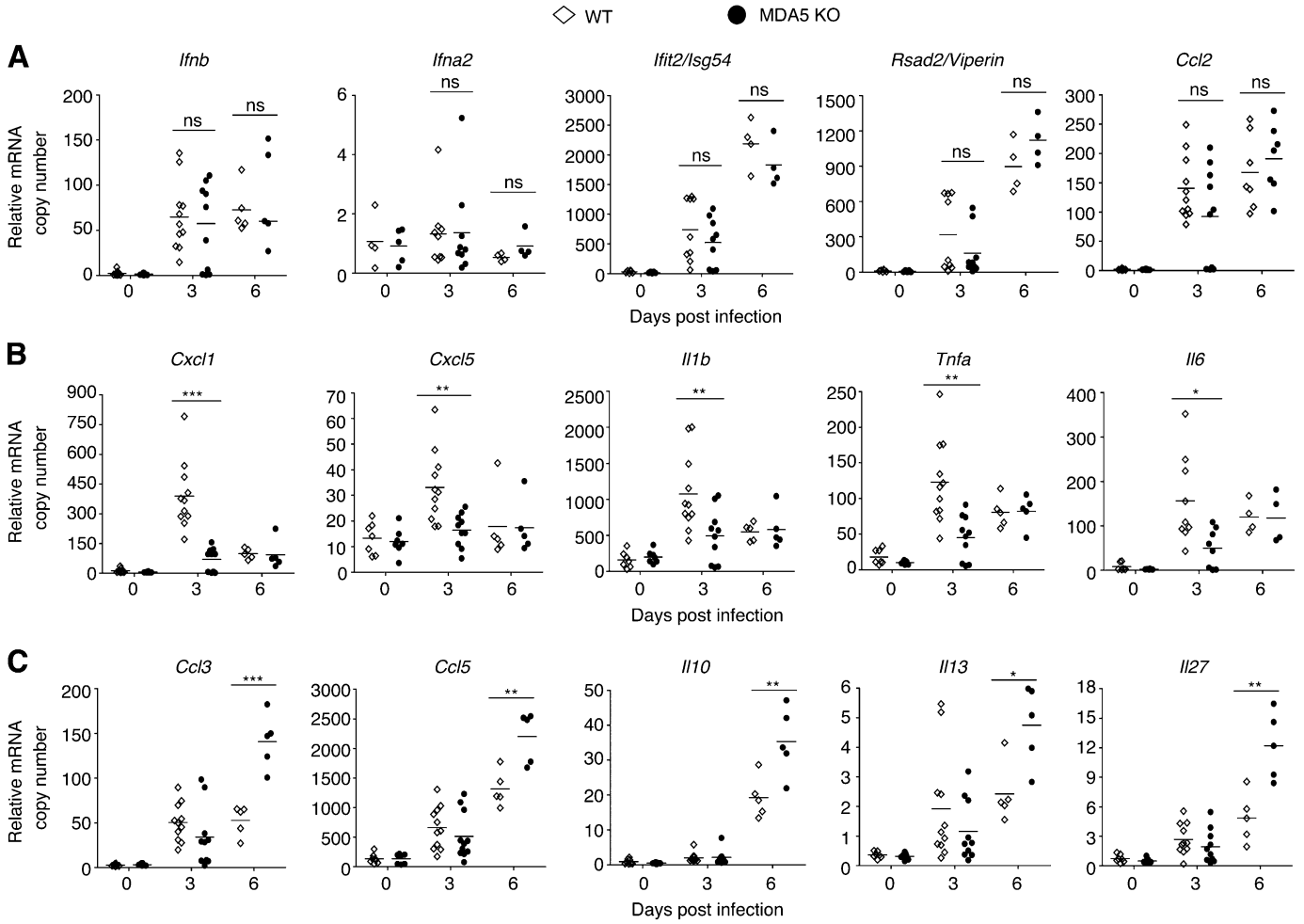

Figure 2. Melanoma differentiation–associated protein 5 (MDA5) modulates the expression of pro- and anti-inflammatory genes during Sendai virus (SeV) infection. Wild-type (WT) and MDA5 knockout (KO) mice were infected with 10 ID_{50} of SeV. Total RNA was extracted at the indicated time points and analyzed by quantitative RT-PCR for the expression of *Ifnb*, *Ifna2*, *Ifit2/Isg54*, and *Rsad2/viperin*, *Ccl2* (*A*); *Cxcl1*, *Cxcl5*, *Il1b*, *Tnfa*, and *Il6* (*B*); and *Ccl3*, *Ccl5*, *Il10*, *Il13*, and *Il27* (*C*). $^*P < 0.05$, $^{**}P < 0.01$, and $^{***}P < 0.001$ (unpaired Student's *t* test). ns = nonsignificant.

lung epithelial cell barrier, protein concentration and cell numbers were determined in the BAL fluid of infected mice. At 10 days after infection, infected MDA5 KO mice had significantly higher protein concentration (Figure 1C) and total cell numbers (Figure 1D) in the BAL compared with infected WT mice, suggesting increased damage and disruption of the epithelial cell barrier. These results demonstrate that MDA5 protects the lung from acute damage during SeV infection by a mechanism that is not dependent on the control of virus replication.

MDA5 Deficiency Results in an Altered Chemokine and Cytokine Profile in the Lung after Virus Infection

We next profiled the expression of antiviral molecules, chemokines, and cytokines in whole lung homogenates from WT and MDA5 KO mice during the course of infection with SeV. Expression of *Ifnb* mRNA as well as expression of a number of molecules with antiviral activity, including *Ifna2*, *Ifit2/Isg54*, and *Rsad2/viperin*, were comparable in WT and MDA5 KO mice (Figure 2A), suggesting that expression of these genes is primarily controlled by other PRRs. However, we observed striking temporal differences on the expression of chemokines and cytokines in the lungs of infected mice. On Day 3 after infection, MDA5 KO mice showed severely reduced expression of the neutrophil-attracting chemokines *Cxcl1* and *Cxcl5* and of the proinflammatory cytokines *Il1b*, *Tnfa*, and *Il6* (Figure 2B), but on Day 6 after infection, MDA5 KO mice exhibited drastically enhanced expression of the monocyte/lymphocyte-attracting chemokines *Ccl3* and *Ccl5* but not of *Ccl2*. In addition, MDA5-deficient mice had increased expression of the regulatory cytokines *Il10*, *Il13*, and *Il27* (Figure 2C). MDA5 did not regulate the expression of *Il33*, *Tslp/Thymic stromal lymphopoietin*, *Areg/Amphiregulin*, or *Il22*, which have been associated with lung tissue repair during respiratory virus infection (25, 26), and transcripts for the granulopoietic cytokine *Cfs3/Gscf* were not different in WT and MDA5 KO mice on Day 3 after infection but were up-regulated in MDA5KO mice on Days 6 and 10 after infection (*see* Figure E1 in the online supplement).

MDA5 Regulates Chemokine Expression by Lung Hematopoietic and Nonhematopoietic Cells

To determine whether the lung hematopoietic and/or nonhematopoietic cellular compartments were influenced by MDA5 signaling, we evaluated *Cxcl1* and *Cxcl5* expression in lung cells isolated 3 days after infection and enriched based on the expression of the hematopoietic marker CD45. Enrichment resulted in 80 to 90% purity of the $CD45^+$ and $CD45^-$ cells. Gating of the enriched cell preparations can be seen in Figure E2. Although most of the SeV *Np* transcripts were found on $CD45^-$ cells on WT and MDA5 KO mice (Figure 3A), $CD45^+$ cells also expressed SeV *Np*. As expected, *Ifng* was expressed only in hematopoietic cells ($CD45^+$) (Figure 3B). *Cxcl1* and *Cxcl5* were predominantly expressed in a MDA5-dependent manner by hematopoietic ($CD45^+$) and nonhematopoietic cells ($CD45^-$) (Figures 3C and 3D), indicating that MDA5 regulates the expression of proinflammatory genes by both cell populations in the lung.

MDA5 Regulates *Cxcl1* Expression through a MAVS-mediated Pathway

To more directly assess the role of MDA5 in chemokine expression, we infected WT and MDA5 KO bone marrow–derived dendritic cells with SeV, influenza A virus (IAV) PR8, or IAV PR8 delNS1 as a control for a RIG-I–dependent virus (15). IAV delNS1 lacks the virus-encoded immune antagonistic protein NS1, allowing the development of a stronger host response to infection (27). After 6 hours, total RNA was extracted from infected cells and analyzed by RT-qPCR. As expected, *Ifih1/Mda5* transcripts were only observed in WT cells, whereas WT and MDA5 KO cells induced comparable levels of *Ddx58/Rig-I* mRNA (Figure 4A). During infection with SeV, MDA5 KO cells showed normal expression of viral *Np* mRNA and of *Ifnb* mRNA but a significantly reduced expression of the neutrophil-attracting chemokine *Cxcl1* mRNA (Figure 4B), demonstrating that MDA5 regulates the expression of the neutrophil-attracting chemokine *Cxcl1* by DCs, whereas other PRRs are responsible

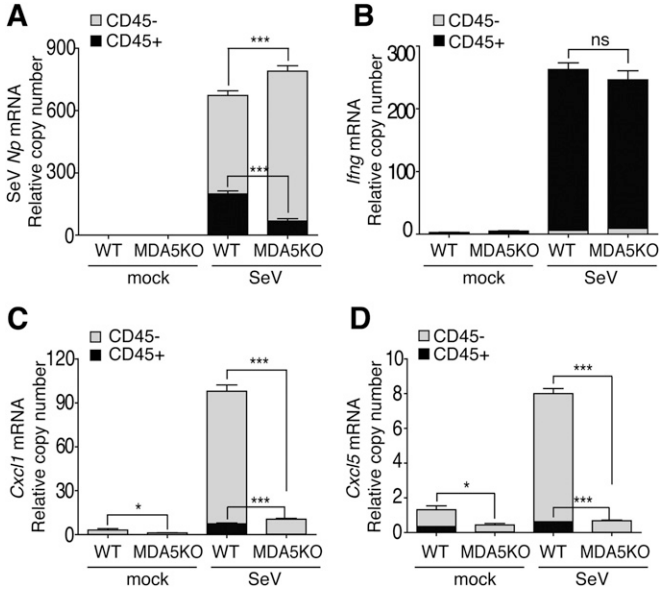

Figure 3. Melanoma differentiation–associated protein 5 (MDA5) regulates the expression of neutrophil-attracting chemokines in hematopoietic ($CD45^+$) and nonhematopoietic ($CD45^-$) cells. Wild-type (WT) and MDA5 knockout (KO) mice were infected with 10 ID_{50} of Sendai virus (SeV) 52. $CD45^+$ and $CD45^-$ cells were enriched after staining. Total RNA was extracted from $CD45^+$ or $CD45^-$ lung cells and analyzed on Day 6 after infection by quantitative RT-PCR for the expression of *SeV Np* (Day 3) (*A*), *Ifng* (Day 6) (*B*), *Cxcl1* (Day 3) (*C*), and *Cxcl5* (Day 3) (*D*). Data are representative of two independent experiments. Height of the *bars* corresponds to the relative copy number in the whole lung. *Black sections* indicate the relative copy number in the $CD45^+$ fraction of the lung, and *gray sections* correspond to the expression of the $CD45^-$ fraction of the lung. *Asterisks* indicate significant differences for each cellular fraction: $^*P < 0.05$ and $^{***}P < 0.001$ (unpaired Student's *t* test). ns = nonsignificant.

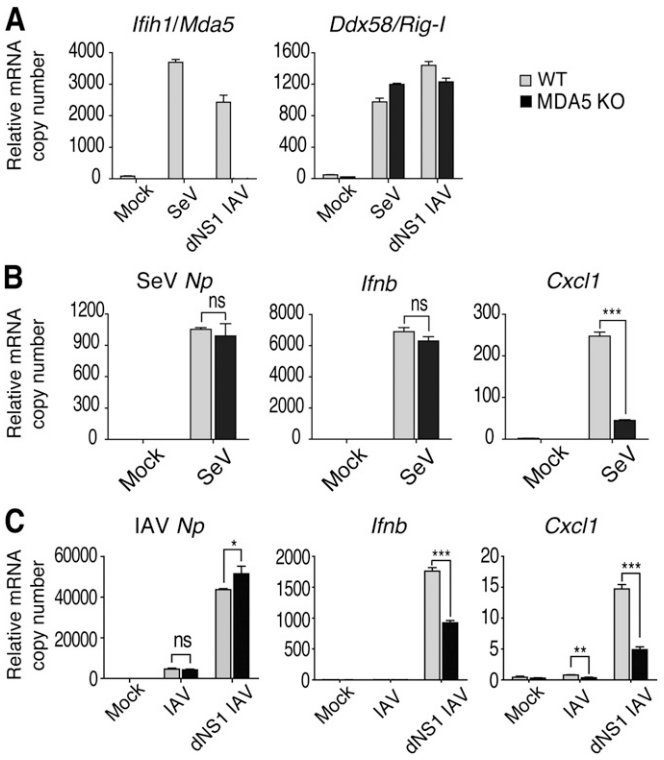

Figure 4. Melanoma differentiation–associated protein 5 (MDA5) plays a critical role in the expression of Cxcl1 in response to respiratory virus infection. Wild-type (WT) and MDA5 knockout (KO) bone marrow–derived cells were infected with multiplicity of infection of 1.5 $TCID_{50}$/cell of Sendai virus (SeV), influenza A virus (IAV), or IAV delNS1. (*A*) After 6 hours, total RNA was analyzed for the expression of *Ifih1/Mda5* and *Ddx58/Rig-I*. Viral protein transcripts, as well as *Ifnb*, and *Cxcl1* mRNA were examined in SeV-infected (*B*) and IAV-infected cells (*C*). *Error bars* indicate the standard deviation of triplicate measurements in a representative experiment. $^*P < 0.05$, $^{**}P < 0.01$, and $^{***}P < 0.001$ (unpaired Student's *t* test). ns = nonsignificant.

for the expression of *Ifnb* mRNA during infection with SeV. Unexpectedly, we observed significantly reduced expression of *Ifnb* and *Cxcl1* transcripts in MDA5 KO cells infected with IAV delNS1 accompanied with an increased expression of IAV *Np* mRNA compared with WT cells (Figure 4C). However, infection with IAV PR8 did not show up-regulation of *Ifnb* and *Cxcl1* transcripts due to the activity of NS1. These results indicate that MDA5 also contributes to the expression of *Cxcl1* and *Ifnb* during infection with IAV delNS1.

To determine whether the RIG-I–like receptors adaptor protein MAVS was required for *Cxcl1* expression in response to SeV or IAV delNS1, we infected WT and MAVS KO mouse embryonic fibroblasts (MEFs) (Figure 5A). Although SeV *Np* mRNA was expressed at high levels in the absence of MAVS and its expression was increased in a dose-dependent manner (Figure 5B), expression of *Ifnb* and *Cxcl1* was completely dependent on the presence of MAVS at all tested doses (Figures 5C and 5D). Similarly, expression of IAV *Np* mRNA was higher in MAVS KO MEFs compared with WT MEFs (Figure 5E), and expression of *Ifnb* and *Cxcl1* transcripts was dependent on MAVS in response to IAV delNS1 (Figures 5F and 5G). These data suggest that MDA5/MAVS-mediated signaling is required for the expression of *Cxcl1* in response to SeV or IAV infection.

MDA5 Modulates the Composition of the Lung Immune Cellular Infiltrate

Based on the differential profile of chemokine expression in infected WT and MDA5 KO mice, we hypothesized that MDA5 deficiency results in an altered composition of infiltrating inflammatory cells in the infected lung. To test this hypothesis, we characterized the cells present in the BAL of WT and MDA5 KO mice 6 days after infection. The gating strategy used for analysis of cell populations is shown in Figure E3. Corresponding with the profile of chemokine expression (Figure 2), significantly fewer neutrophils infiltrated the lungs of MDA5 KO mice on Day 6 after infection (Figure 6A), associated with a lower percentage of $Ly6G^{high}$ granulocytic cells and a higher percentage of $Ly6C^{high}$ monocytic cells in the lung infiltrate of MDA5 KO mice compared with WT controls (Figures 6B and 6C). In addition, BAL of MDA5 KO mice had a higher percentage of $CD3^+$ T cells at this time point. Although we did not directly address in this study whether these T cells were predominantly of a Th2 type, we did observe an increase in the content of $CD4^+$ and $CD8^+$ T cells in the lung of MDA5-deficient mice (not shown), suggesting and overall enhancement on the T-cell response at this time point. In WT and MDA5 KO mice, resident alveolar macrophages characterized as $CD11b^{int/low}F4/80^+CD11c^+CD206^+$ cells (Figure E4) disappeared by Day 6 after infection (Figure 6D) and were replaced by $CD11b^{hi}$-expressing cells. By Day 21 after infection, infected MDA5 KO mice showed a higher percentage of cells expressing markers of alternatively activated macrophages (AAMs: $CD11b^{high}F4/80^+CD11c^+CD206^+$). Based on the shift in the proinflammatory profile of the lung toward the expression of *Il10* and *Il13* and on reports demonstrating a critical role for AAMs in the development of chronic lung diseases in response to SeV (7), we hypothesized that MDA5 deficiency resulted in the excessive accumulation of pathogenic AAMs, leading to the exacerbation of chronic lung disease. Supporting this hypothesis, MDA5 KO mice exhibited a significantly higher ratio of *Arg1/Nos2* (28) mRNA expression than WT mice at 10 and 21 days after infection (Figure 6E) and expressed more transcripts for *Mmp12*, *Relmα/Fizz1*, and *Chi3l3/4/Ym1/2*, although the difference did not always reach statistical significance at these time points. To confirm the bias toward AAMs in MDA5 KO mice, lungs from mice infected for 49 days were stained for FIZZ1, YM1, and F4/80 proteins, the standard markers of AAMs. Both proteins were expressed at much higher

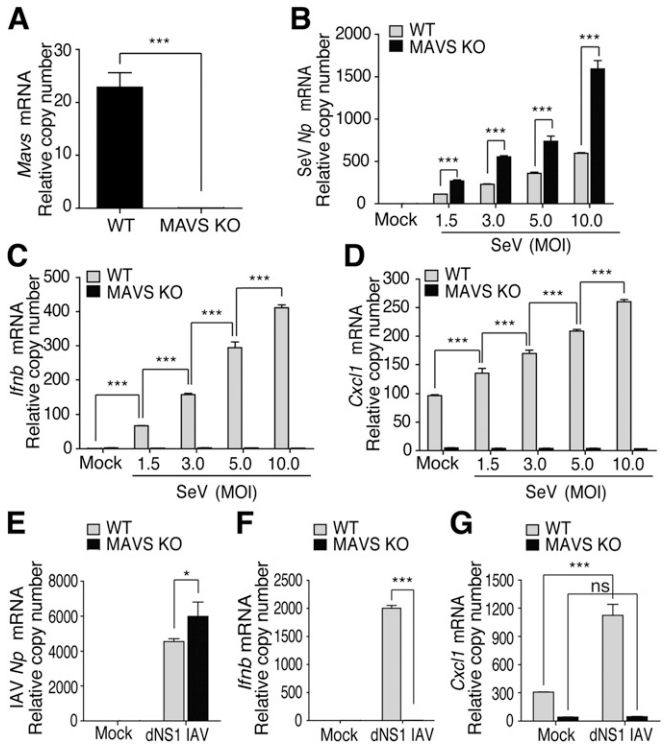

Figure 5. Mitochondrial antiviral-signaling protein (MAVS) is essential for the expression of Cxcl1 upon Sendai virus (SeV) or influenza A virus (IAV) infection. Wild-type (WT) and MAVS knockout (KO) mouse embryonic fibroblasts (MEFs) were infected with different multiplicity of infection (MOI) doses of SeV (*A–D*) or MOI of 1.5 $TCID_{50}$/cell of delNS1 influenza A virus (IAV) (*E–G*). After 6 hours, total RNA was analyzed for the expression of *Mavs* (*A*), *SeV Np* (*B*), *IAV Np* (*E*), *Ifnb* (*C*, *F*), and *Cxcl1* (*D*, *G*). *Error bars* indicate the standard deviation of triplicate measurements in a representative experiment. $^*P < 0.05$ and $^{***}P < 0.001$ (unpaired Student's *t* test). ns = nonsignificant.

levels in MDA5 KO than in infected WT lungs, corresponding with the expression of F480 (Figure 7) and demonstrating a persistent AAM bias in the absence of MDA5. These data strongly suggest that MDA5 signaling determines the acute composition of the lung cellular infiltrate and regulates the persistent accumulation of AAMs during SeV infection.

MDA5 Protects from Postviral Chronic Airway Inflammation

To determine the impact of MDA5 on chronic postviral inflammation, we analyzed hematoxylin and eosin–stained lung tissue sections on Days 21 and 49 after infection. MDA5-deficient mice showed exacerbated alveolar congestion and peribronchial inflammation compared with WT mice. Histopathologic scoring (described in the legend of Figure 8) revealed enhanced total histopathology and mildly enhanced bronchial smooth muscle hyperplasia in infected MDA5-deficient mice compared with infected WT mice (Figures 8A and 8B). Augmented Goblet cell hyperplasia and mucus production were also observed in MDA5 KO mice lungs (Figure 8C). These results suggest that MDA5-deficient mice are susceptible to exacerbated virus-induced lung injury and that MDA5 protects from the development of chronic airway inflammation.

To determine the chronic impact of MDA5 deficiency on pulmonary function, we measured Sp_{O_2} in mock- and SeV-infected mice on Day 49 after infection. Mean Sp_{O_2} values in mock-infected WT and MDA5 KO mice were 94.9% (range, 89.7–98.8%) and 96.3% (range, 92.5–99.1%), respectively. Both groups showed a significant decrease in arterial oxygen saturation after 49 days of infection (Figure 8D). Conversion of Sp_{O_2} to Pa_{O_2} from the oxyhemoglobin dissociation curve revealed a significant decrease in Pa_{O_2} in infected MDA5-deficient mice, whereas the decrease in Pa_{O_2} did not reach statistical significance in WT mice (Figure 8E). These data suggest that the decreased pulmonary function observed chronically after SeV infection is worse in the absence of MDA5, corresponding with the observed enhanced inflammation and goblet cell hyperplasia.

Airway hyperreactivity is a common manifestation of chronic postviral lung disease in susceptible individuals. To assess the impact of MDA5 on airway hyperreactivity, we measured contractility of the airways in response to increasing doses of carbachol (10^{-8} to 10^{-4} M). Using precision-cut lung slices, enhanced constriction was observed in the lung from infected WT and KO groups on Day 21 after infection (Figure 8F) with a log half maximal effective concentration of carbachol of -0.4130 ± 0.1159 for infected WT lungs and 0.02296 ± 0.1168 for MDA5 KO lungs ($P = 0.0083$ by unpaired *t* test). This hyperreactivity was only sustained in MDA5 KO lungs by Day 49 after infection (Figures 8G–8I) with a log half maximal effective concentration value of 0.3982 ± 0.1855 for infected WT lungs and -0.01175 ± 0.07523 for MDA5 KO lungs ($P = 0.0180$ by unpaired *t* test). At this time point, airways from SeV-infected MDA5 KO mice demonstrated a significant increase in maximal bronchoconstriction (Figure 8I) and area under the curve (Figure 8H) in response to carbachol. These data demonstrate that MDA5 deficiency leads to chronic airway hyperreactivity after SeV infection.

Discussion

In this study we describe a novel immunomodulatory function of the intracellular helicase MDA5 in response to paramyxovirus infection. MDA5 deficiency results in altered expression of chemokines and cytokines in the infected lung and in differential composition of the lung inflammatory infiltrate, leading to exacerbated chronic lung pathology. MDA5 KO mice exhibited pulmonary neutropenia associated with reduced expression of the neutrophil-attracting chemokines *Cxcl1* and *Cxcl5* and increased accumulation of AAMs. This cellular composition correlated with enhanced expression of the monocyte/lymphocyte-attracting chemokines *Ccl3*

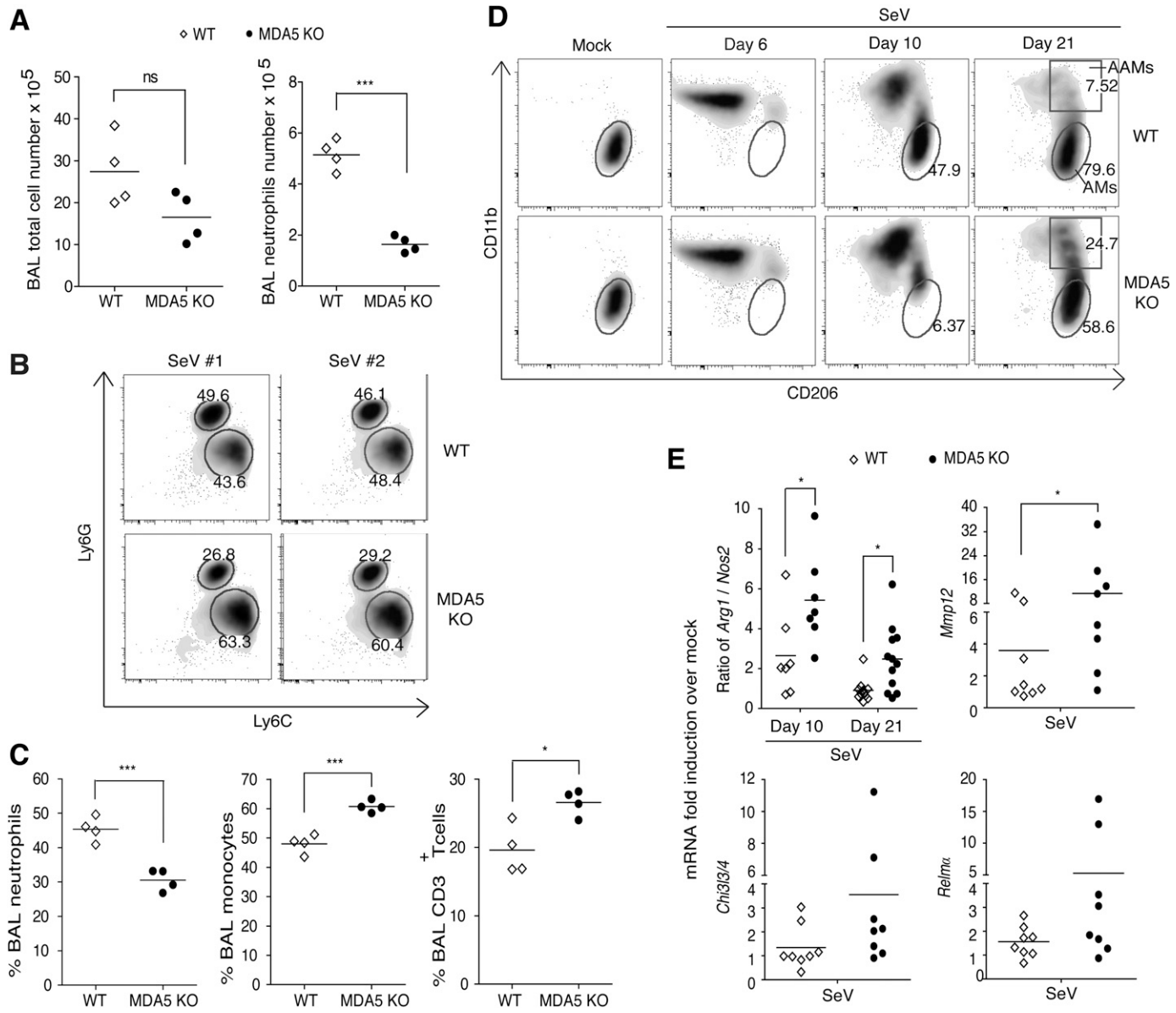

Figure 6. Melanoma differentiation–associated protein 5 (MDA5) deficiency elicits an altered composition of the inflammatory cellular infiltrate upon Sendai virus (SeV) infection. Wild-type (WT) and MDA5 knockout (KO) mice were infected with 10 ID_{50} of SeV 52. Single-cell suspensions isolated from bronchoalveolar lavage (BAL) of WT and MDA5 KO infected mice at the indicated time points were analyzed by flow cytometry. (*A*) Total and neutrophil cell counts. (*B*) Representative plots for $CD11b^{high}Ly6G^{+}$ granulocytes and $CD11b^{high}Ly6C^{+}$ monocytes are shown. Cells were pregated on live, singlets, and $CD45^{+}$. Samples of two infected animals for each WT and MDA5 KO mice are shown. (*C*) Percentage of $CD11b^{+}Ly6G^{+}$ (neutrophils) cells, $CD11b^{+}Ly6C^{+}$ (monocytes) cells, and $CD3^{+}$ T cells. (*D*) Single-cell suspensions from WT and MDA5 KO infected lungs were prepared on Days 6, 10, 21, and 49 after infection. Cells were pregated on live, singlets, $CD11c^{+}$, and $F4/80^{+}$ cells. Alternatively activated macrophages (AAMs) ($CD11b^{high}F4/80^{+}CD11c^{+}CD206^{+}$) and alveolar macrophages (AMs) ($CD11b^{int/low}F4/80^{+}CD11c^{+}CD206^{+}$) are shown. (*E*) Total RNA was extracted from WT and MDA5 KO infected lungs at the indicated times. Ratio of *Arg1/Nos2* mRNA was determined by quantitative RT-PCR. Expression of *Mmp12*, *Relmα/Fizz1*, and *Chi3l3/4/Ym1/2* was examined from RNA in lungs infected on Day 21 after infection (n = 4–12). $^{*}P < 0.05$; $^{***}P < 0.001$ (unpaired Student's *t* test for % cells and unpaired Mann-Whitney test for fold induction).

and *Ccl5* and of the immunoregulatory cytokines *Il10*, *Il13*, and *Il27* as well as with exacerbated postviral chronic airway inflammation.

Neutrophils are typically the first cells recruited to the lung during viral or bacterial infections (29) and produce immune mediators, such as TNF-α and IL-1β, that enhance the inflammatory response (30, 31). Phagocytosis of apoptotic neutrophils by tissue macrophages promotes resolution of inflammation after infection (32, 33). Using G-CSF KO mice, we previously reported that neutrophil deficiency led to the enhanced expression of *Ccl3* and *Ccl5* during SeV infection (34). MDA5 KO mice showed lung neutropenia and accumulation of $CD11b^{high}F4/80^{+}CD11c^{+}CD206^{+}$

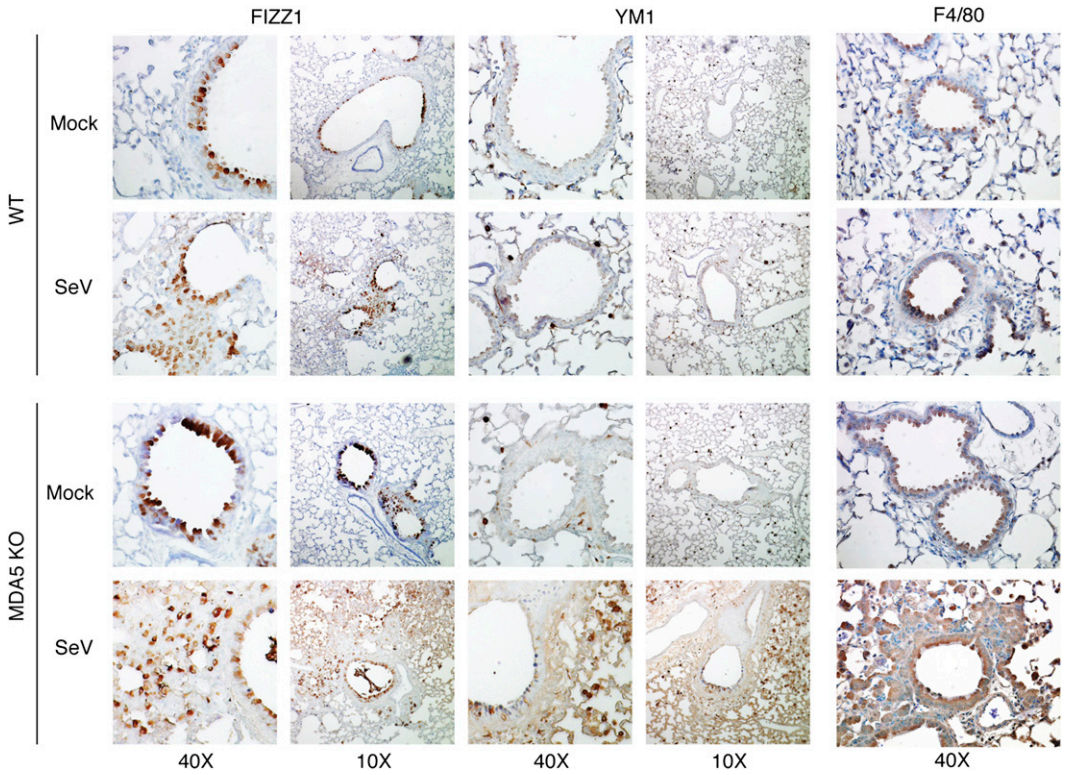

Figure 7. The alternatively activated macrophage markers FIZZ1, YM1, and F480 are highly expressed in the lung of melanoma differentiation–associated protein 5 (MDA) knockout (KO) mice infected with Sendai virus (SeV) for 49 days. Wild-type (WT) and MDA5 KO mice were infected with 10 ID_{50} of SeV 52. After 49 days, lung tissues were analyzed by immunohistochemistry. The tissues were stained for FIZZ1, YM1, and F480. Original magnification: ×10 and ×40 for FIZZ1 and YM1; 40× for F4/80.

cells; enhanced expression of the immunomodulatory cytokines *Il10*, *Il13*, and *Il27*; a higher ratio of *Arg1*/*Nos2*; and higher expression of *Mmp12*, *Fizz1*, and *Ym1/2* compared with WT controls, all indicative of the accumulation of AAMs. Chronic lung inflammation upon SeV infection is mediated by the accumulation of AAMs (7), suggesting that their enhanced accumulation in MDA5-deficient mice is responsible for increased pathology. Resident alveolar macrophages ($CD11b^{low}F4/80^{+}CD11c^{+}CD206^{+}$) that disappear from the lung immediately after infection were replenished more efficiently in WT than in MDA5 KO mice, agreeing with physiological and histologic data demonstrating delayed recovery from infection in MDA5 KO mice.

The molecular mechanisms regulating the accumulation and function of macrophages are not well understood, but it is likely that reduced numbers of apoptotic neutrophils affect the differentiation and activation of lung macrophages (32, 33). Apoptotic neutrophils up-regulate the CCL3/CCL5 receptor CCR5, and increased CCR5 on neutrophils thereby sequesters the chemokine CCL3 and CCL5, resulting in the resolution of inflammation (35). Thus, it is possible that reduced neutrophil recruitment to the lung in MDA5 KO mice leads to excessive levels of CCL3 and CCL5 and to enhanced activity of AAMs (36, 37). Alternatively, and not exclusively, lipid mediators produced upon uptake of apoptotic neutrophils may affect the differentiation and function of macrophages, as it has been shown in a murine peritonitis model (38).

We showed that MDA5 deficiency did not affect the expression of an important subset of type I IFNs or of type I IFN–responsive genes and that SeV replication and clearance occurred normally in the absence of MDA5. These data suggest that other PRRs are primarily responsible for the control of virus replication during low-dose SeV infection, in contrast to a previous study that uses a higher SeV inoculum. In striking contrast, expression of *Cxcl1* is largely dependent on MDA5 during infection with SeV, influenza PR8 virus, or influenza delNS1 virus, suggesting that, contrary to current paradigms, MDA5 and RIG-I have distinct nonredundant roles during the response to these viruses.

SeV-infected MDA5 KO mice showed a statistically significant reduction in arterial Pa_{O_2} compared with infected WT mice. An acute fall in Pa_{O_2} or a Sp_{O_2} of less than 85 to 88% indicate a significant loss of oxygen homeostasis and loss of biological oxygenation reserve. The increased inability of MDA5 KO mice to maintain blood oxygenation, together with pathophysiological alterations, demonstrate that MDA5 deficiency promotes chronic pulmonary dysfunction. In addition, MDA5 deficiency leads to sustained airway hyperreactivity, corresponding with enhanced bronchial smooth muscle hyperplasia, a characteristic of asthmatic airways. Because airway hyperreactivity is a common manifestation of chronic disease in individuals infected

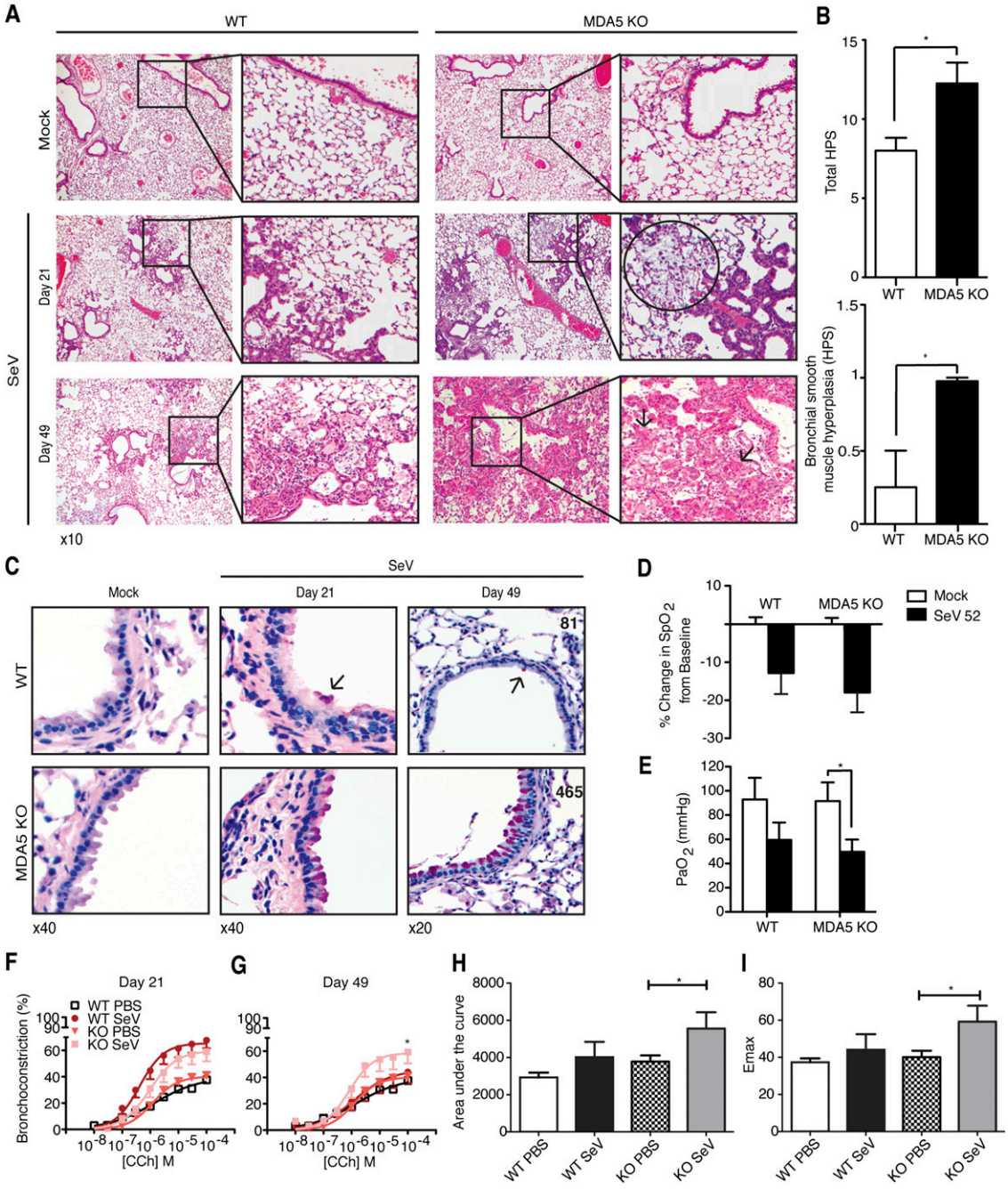

Figure 8. Melanoma differentiation–associated protein 5 (MDA5) deficiency exacerbates chronic airway inflammation and pathology. Wild-type (WT) and MDA5 knockout (KO) mice were infected with 10 ID_{50} of Sendai virus (SeV) 52. (*A*) Lungs were collected on Days 21 and 49 after infection and analyzed by hematoxylin and eosin staining. The *circle* indicates accumulation of mucus in the alveolar space. *Arrows* indicate eosinophilic crystals. Original magnification: ×10. (*B*) Histologic scores are indicated and represent mean ± SD for four mice. Total histopathologic score (HPS) includes bronchiolar/alveolar epithelial hyperplasia (% of terminal bronchioles affected), alveolar epithelial hyperplasia (extent of area affected on most severe focus), bronchiolar smooth muscle hyperplasia, eosinophilic macrophage crystals, and inflammation. $^*P < 0.05$ (unpaired one-tailed Mann-Whitney test). (*C*) Periodic acid-Schiff (PAS) staining on 21- and 49-day–infected lungs. *Arrows* indicate goblet cells positive for PAS (n = 3–6 per group). Number of PAS-positive cells for Day 49 is indicated. (*D*) Percentage change in oxygen saturation levels (Sp_{O_2}) as determined by pulse-oxymetry (*top*) (n = 4). (*E*) Pa_{O_2} as estimated through Ventworld interactive oxyhemoglobin dissociation curve (*bottom*). Data correspond to Day 49 after infection. $^*P < 0.05$ by one-way ANOVA. (*F–I*) Lungs from WT and MDA5 KO mice exposed to SeV were sliced to examine contractility of the airways. Slices from mice infected for 21 days (*F*) or 49 days (*G–I*) were exposed to increasing doses of carbachol (10^{-8} to 10^{-4} M), and percent of bronchoconstriction was determined by measuring the airway lumen and comparing it with the baseline area of the airway. (*H*) Mean ± SEM of area under the curve on Day 49. (*I*) Maximal constriction (Emax) values derived from the Day 49 concentration response curve. Data correspond to 3 to 8 mice and 9 to 23 slices per treatment group. Results were analyzed using one-way ANOVA with Bonferroni's post test, with $^*P < 0.05$ considered significant.

with paramyxoviruses, including respiratory syncytial virus, parainfluenza virus, and metapneumovirus (39–41), it would be interesting to determine whether polymorphisms in the MDA5 molecule correlate with enhanced susceptibility to chronic postviral lung diseases.

In conclusion, we demonstrate that MDA5 modulates the lung inflammatory response induced by SeV infection and protects from the development of severe chronic lung pathology. MDA5-associated signaling and downstream events may provide novel targets for therapeutic intervention in individuals susceptible to the development of postviral chronic lung inflammation. ■

Author disclosures are available with the text of this article at www.atsjournals.org.

Acknowledgment: The authors thank Drs. Jonathan C. Kagan (Harvard), Marco Colonna, Michael S. Diamond (Washington University), Adolfo García-Sastre (Icahn School of Medicine at Mount Sinai), and Susan Weiss (University of Pennsylvania) for providing invaluable reagents; Jonathan Brestoff for support with flow cytometry; the Flow Cytometry and Cell Sorting Resource Laboratory at the University of Pennsylvania; and Karla Tapia for valuable technical support.

References

1. Yamaya M. Virus infection-induced bronchial asthma exacerbation. *Pulm Med* 2012;2012:834826.
2. Proud D, Chow CW. Role of viral infections in asthma and chronic obstructive pulmonary disease. *Am J Respir Cell Mol Biol* 2006;35: 513–518.
3. Meneghin A, Hogaboam CM. Infectious disease, the innate immune response, and fibrosis. *J Clin Invest* 2007;117:530–538.
4. Umetsu DT, Dekruyff RH. Natural killer T cells are important in the pathogenesis of asthma: the many pathways to asthma. *J Allergy Clin Immunol* 2010;125:975–979.
5. Chang YJ, Kim HY, Albacker LA, Baumgarth N, McKenzie AN, Smith DE, Dekruyff RH, Umetsu DT. Innate lymphoid cells mediate influenza-induced airway hyper-reactivity independently of adaptive immunity. *Nat Immunol* 2011;12:631–638.
6. Kim HY, Chang YJ, Subramanian S, Lee HH, Albacker LA, Matangkasombut P, Savage PB, McKenzie AN, Smith DE, Rottman JB, *et al*. Innate lymphoid cells responding to IL-33 mediate airway hyperreactivity independently of adaptive immunity. *J Allergy Clin Immunol* 2012;129:216–227, e1–e6.
7. Kim EY, Battaile JT, Patel AC, You Y, Agapov E, Grayson MH, Benoit LA, Byers DE, Alevy Y, Tucker J, *et al*. Persistent activation of an innate immune response translates respiratory viral infection into chronic lung disease. *Nat Med* 2008;14:633–640.
8. Holtzman MJ, Patel DA, Zhang Y, Patel AC. Host epithelial-viral interactions as cause and cure for asthma. *Curr Opin Immunol* 2011;23:487–494.
9. Page C, Goicochea L, Matthews K, Zhang Y, Klover P, Holtzman MJ, Hennighausen L, Frieman M. Induction of alternatively activated macrophages enhances pathogenesis during severe acute respiratory syndrome coronavirus infection. *J Virol* 2012;86:13334–13349.
10. Agapov E, Battaile JT, Tidwell R, Hachem R, Patterson GA, Pierce RA, Atkinson JJ, Holtzman MJ. Macrophage chitinase 1 stratifies chronic obstructive lung disease. *Am J Respir Cell Mol Biol* 2009;41: 379–384.
11. Swiecki M, Colonna M. Type I interferons: diversity of sources, production pathways and effects on immune responses. *Curr Opin Virol* 2011;1:463–475.
12. Ireton RC, Gale M Jr. RIG-I like receptors in antiviral immunity and therapeutic applications. *Viruses* 2011;3:906–919.
13. Yount JS, Gitlin L, Moran TM, Lopez CB. MDA5 participates in the detection of paramyxovirus infection and is essential for the early activation of dendritic cells in response to Sendai Virus defective interfering particles. *J Immunol* 2008;180:4910–4918.
14. Gitlin L, Benoit L, Song C, Cella M, Gilfillan S, Holtzman MJ, Colonna M. Melanoma differentiation-associated gene 5 (MDA5) is involved in the innate immune response to Paramyxoviridae infection in vivo. *PLoS Pathog* 2010;6:e1000734.
15. Loo YM, Fornek J, Crochet N, Bajwa G, Perwitasari O, Martinez-Sobrido L, Akira S, Gill MA, Garcia-Sastre A, Katze MG, *et al*. Distinct RIG-I and MDA5 signaling by RNA viruses in innate immunity. *J Virol* 2008;82:335–345.
16. Kato H, Takeuchi O, Sato S, Yoneyama M, Yamamoto M, Matsui K, Uematsu S, Jung A, Kawai T, Ishii KJ, *et al*. Differential roles of MDA5 and RIG-I helicases in the recognition of RNA viruses. *Nature* 2006; 441:101–105.
17. Wang W, Nguyen NM, Agapov E, Holtzman MJ, Woods JC. Monitoring in vivo changes in lung microstructure with (3)He MRI in Sendai virus-infected mice. *J Appl Physiol* 2012;112:1593–1599.
18. Kim WK, Jain D, Lopez CB. MDA5 protects from the development of long-term chronic airway inflammation during respiratory viral infections [abstract]. Presented at the Keystone Symposium: The Innate Immune Response in the Pathogenesis of Infectious Disease. Ouro Preto, Brazil, May 10–15, 2013.
19. Mercado-Lopez X, Cotter CR, Kim WK, Sun Y, Munoz L, Tapia K, Lopez CB. Highly immunostimulatory RNA derived from a Sendai virus defective viral genome. *Vaccine* 2013;31:5713–5721.
20. Tapia K, Kim WK, Sun Y, Mercado-Lopez X, Dunay E, Wise M, Adu M, Lopez CB. Defective viral genomes arising in vivo provide critical danger signals for the triggering of lung antiviral immunity. *PLoS Pathog* 2013;9:e1003703.
21. Lopez CB, Fernandez-Sesma A, Schulman JL, Moran TM. Myeloid dendritic cells stimulate both Th1 and Th2 immune responses depending on the nature of the antigen. *J Interferon Cytokine Res* 2001;21:763–773.
22. Jain D, Atochina-Vasserman EN, Tomer Y, Kadire H, Beers MF. Surfactant protein D protects against acute hyperoxic lung injury. *Am J Respir Crit Care Med* 2008;178:805–813.
23. Davis IC, Lazarowski ER, Chen FP, Hickman-Davis JM, Sullender WM, Matalon S. Post-infection A77–1726 blocks pathophysiologic sequelae of respiratory syncytial virus infection. *Am J Respir Cell Mol Biol* 2007;37:379–386.
24. Cooper PR, Mesaros AC, Zhang J, Christmas P, Stark CM, Douaidy K, Mittelman MA, Soberman RJ, Blair IA, Panettieri RA. 20-HETE mediates ozone-induced, neutrophil-independent airway hyper-responsiveness in mice. *PLoS ONE* 2010;5:e10235.
25. Monticelli LA, Sonnenberg GF, Abt MC, Alenghat T, Ziegler CG, Doering TA, Angelosanto JM, Laidlaw BJ, Yang CY, Sathaliyawala T, *et al*. Innate lymphoid cells promote lung-tissue homeostasis after infection with influenza virus. *Nat Immunol* 2011;12:1045–1054.
26. Pociask DA, Scheller EV, Mandalapu S, McHugh KJ, Enelow RI, Fattman CL, Kolls JK, Alcorn JF. IL-22 is essential for lung epithelial repair following influenza infection. *Am J Pathol* 2013;182: 1286–1296.
27. Wang X, Li M, Zheng H, Muster T, Palese P, Beg AA, Garcia-Sastre A. Influenza A virus NS1 protein prevents activation of NF-kappaB and induction of alpha/beta interferon. *J Virol* 2000; 74:11566–11573.
28. Munder M, Eichmann K, Modolell M. Alternative metabolic states in murine macrophages reflected by the nitric oxide synthase/arginase balance: competitive regulation by CD4+ T cells correlates with Th1/Th2 phenotype. *J Immunol* 1998;160:5347–5354.
29. Kolaczkowska E, Kubes P. Neutrophil recruitment and function in health and inflammation. *Nat Rev Immunol* 2013;13:159–175.
30. Bennouna S, Bliss SK, Curiel TJ, Denkers EY. Cross-talk in the innate immune system: neutrophils instruct recruitment and activation of dendritic cells during microbial infection. *J Immunol* 2003;171: 6052–6058.
31. van Gisbergen KP, Sanchez-Hernandez M, Geijtenbeek TB, van Kooyk Y. Neutrophils mediate immune modulation of dendritic cells through glycosylation-dependent interactions between Mac-1 and DC-SIGN. *J Exp Med* 2005;201:1281–1292.

32. Soehnlein O, Lindbom L. Phagocyte partnership during the onset and resolution of inflammation. *Nat Rev Immunol* 2010;10:427–439.
33. Silva MT. Macrophage phagocytosis of neutrophils at inflammatory/infectious foci: a cooperative mechanism in the control of infection and infectious inflammation. *J Leukoc Biol* 2011;89:675–683.
34. Hermesh T, Moran TM, Jain D, Lopez CB. Granulocyte colony-stimulating factor protects mice during respiratory virus infections. *PLoS ONE* 2012;7:e37334.
35. Ariel A, Fredman G, Sun YP, Kantarci A, Van Dyke TE, Luster AD, Serhan CN. Apoptotic neutrophils and T cells sequester chemokines during immune response resolution through modulation of CCR5 expression. *Nat Immunol* 2006;7:1209–1216.
36. Tyner JW, Uchida O, Kajiwara N, Kim EY, Patel AC, O'Sullivan MP, Walter MJ, Schwendener RA, Cook DN, Danoff TM, *et al*. CCL5–CCR5 interaction provides antiapoptotic signals for macrophage survival during viral infection. *Nat Med* 2005;11:1180–1187.
37. Amulic B, Cazalet C, Hayes GL, Metzler KD, Zychlinsky A. Neutrophil function: from mechanisms to disease. *Annu Rev Immunol* 2012;30:459–489.
38. Schif-Zuck S, Gross N, Assi S, Rostoker R, Serhan CN, Ariel A. Saturated-efferocytosis generates pro-resolving CD11b low macrophages: modulation by resolvins and glucocorticoids. *Eur J Immunol* 2011;41:366–379.
39. Sigurs N, Gustafsson PM, Bjarnason R, Lundberg F, Schmidt S, Sigurbergsson F, Kjellman B. Severe respiratory syncytial virus bronchiolitis in infancy and asthma and allergy at age 13. *Am J Respir Crit Care Med* 2005;171:137–141.
40. Hamelin ME, Prince GA, Gomez AM, Kinkead R, Boivin G. Human metapneumovirus infection induces long-term pulmonary inflammation associated with airway obstruction and hyperresponsiveness in mice. *J Infect Dis* 2006;193:1634–1642.
41. Potena A, Caramori G, Casolari P, Contoli M, Johnston SL, Papi A. Pathophysiology of viral-induced exacerbations of COPD. *Int J Chron Obstruct Pulmon Dis* 2007;2:477–483.